An automated brain tumor detection and classification from MRI images using machine learning techniques with IoT

Article *in* Environment Development and Sustainability · September 2022

DOI: 10.1007/s10668-021-01861-8

CITATIONS
31

READS
674

2 authors:

Anil Kumar Budati
K L University
57 PUBLICATIONS **580** CITATIONS
SEE PROFILE

K. Rajesh Babu
K L University
29 PUBLICATIONS **215** CITATIONS
SEE PROFILE

Environment, Development and Sustainability (2022) 24:10570–10584
https://doi.org/10.1007/s10668-021-01861-8

An automated brain tumor detection and classification from MRI images using machine learning techniques with IoT

Anil Kumar Budati[1] · **Rajesh Babu Katta**[2]

Received: 2 July 2021 / Accepted: 25 September 2021 / Published online: 12 October 2021

Abstract
In medical imaging applications, the accurate diagnosis of brain tumors from magnetic resonance imaging (MRI) at an early stage is a challenging task to researchers nowadays. The early detection of the tumor reduces the mortality rate from brain cancer-related deaths. Among various medical imaging techniques, the MRI is utilized due to low ionization and radiation, but manual inspection takes a lot of time. This proposed work introduces a machine learning technique (MLT) to recognize and classify the tumorous or non-tumorous regions based on the brain MRI dataset. There are four steps to carry out the MLT such as preprocessing, segmentation, feature extraction, and classification procedures. In the first stage, the skull is removed manually to reduce the time complexity by avoiding the process of the unwanted area of the brain image, and median filtering is utilized to filter the noise factor. Next, Chan-Vese (C-V) technique is used to segment the active tumor by selecting the exact initial point. In the very next step, the features of the tumor area are extracted using the gray level co-occurrence matrix (GLCM), and then important statistical features were chosen. Finally, a two-class classifier is implemented using the support vector machine (SVM) and its performance is then validated with k nearest neighbor (KNN). The accomplishment of the proposed flow work was evaluated in terms of accuracy, sensitivity, specificity, and precision by performing on the BRATS 2017 benchmark dataset. The simulation results reveal that the proposed system outer performs over existing methods with high accuracy.

Keywords MLT · Brain tumor · Level–level set · Chan-Vese · GLSM · KNN · SVM

✉ Rajesh Babu Katta
K.9885995375@gmail.com

Anil Kumar Budati
anilbudati@gmail.com

[1] Department of ECE, GRIET, Hyderabad, India

[2] Department of ECE, KLEF, Vijayawada, India

1 Introduction

Cancer is caused by the proliferation of cancerous cells in the human brain, which damages healthy brain cells. The brain tissues were influenced by a variety of parameters, including the size, location, and texture of the brain (Liu et al., 2014). Malignant (cancerous) and benign (non-cancerous) tumors are the two main forms. Malignant tumors are more aggressive and start growing inside brain cells quickly. The benign tumor begins in the body and spreads to the brain's cells (Kapoor & Thakur, 2017; Rohini1ana & Pushpa ani., 2015). Brain tumors are formally classed as cancer in about one-third of cases, making them one of the leading causes of cancer-related death. As a result, initial tissue recognition is necessary to protecting individuals from death. New breakthroughs in medical imaging present clinicians with a solution for future treatment reasons (Ersoz et al., 2017).

For doctors, manual assessment is a time-consuming and repeated procedure. As a result, computerized approaches are necessary to identify a tumor in a short time period and with greater precision (Raju et al. 2019). Several studies have recently proposed a variety of strategies for segmenting the tumor picture from the brain MRI image, including edge, region, segmentation based on cluster, super pixels, fusion-based and optimization, and so on (Masood et al., 2015; Nagajaneyulu & Satya Prasad, 2021). However, due of the differences in tumor boundary, shape, irregularity, and texture in brain images, there are various obstacles. However, these systems have a variety of problems that affect their accuracy (Chakraborty et al. 2018). The size, shape, location, and irregularity of the tumor are all key issues. To address these issues, this research proposes automated brain tumor identification and classification using MRI images utilizing MLT for accurate tumor identification. "The foremost objective is to study the MLT by comparing classifiers namely, SVM and KNN techniques to classify the tumor whether it is cancerous or benign and examine the efficacy of the introduced brain tumor detection system." The rest of the manuscript is broken down into four sections: Sect. 2 summarizes previous work, Sect. 3 introduces the proposed brain tumor segmentation method, Sect. 4 examines simulation findings and discusses them, and Sect. 5 concludes.

2 Related work

Lankton et al. provided a framework for localization that may be used for localization of any region-based energy (Lankton & Tannenbaum, 2008). Though localization can tolerate intensity in homogeneity, the loss of global characteristics makes the initial contour placements more sensitive. To circumvent the difficulty of tapping into local minima, certain global minimization active contour models have recently been presented. The C–V model's convex relaxation approach was proposed by Chan et al. (Chan et al., 2006). Bresson et al. (2007) went on to mention that the active contour/snake model has a global minimization.

Li et al. (2011) suggested a variational level-set framework for correction of bias and segmentation of image with intensity-based inhomogeneity. As a result, segmentation and bias field estimate are carried out in tandem by reducing the suggested energy functional. Our variational framework's data term assures that the bias field derived from the suggested energy has a slow-varying characteristic. On the bias field, there is no need to provide an explicit smoothing term.

Remya Ajai and Gopalan (2020) proposed the active contours segmentation without edge approach toward classification of brain tumor with SVM and KNN classifiers. The authors used several preprocessing techniques for picture augmentation, such as image sharpening and contrast stretching, before executing the active contour without edge-based segmentation. The accuracy of both conventional SVM and KNN classifiers is evaluated whenever active contouring excepting "edge method" of segmentation is utilized, and it is discovered that KNN is considerably more suitable for segmentation of brain tumor than SVM. However, this method was unable to detect the tumor's shapeless growth.

Vijji and Hein Rajesh (2020) introduced a method for classifying MRI images of Brain based on segmentation and classifier of the type KNN. First, the original images were preprocessed utilizing Gaussian filter and then normalized. Next, the normalized images were applied to TIORGW technique (Texture and Intensity-Oriented Region GroWing) and then algorithm of genetic is utilized to retrieve the optimal texture features. Next, the optimum characteristics are supplied to the KNN classifier to classify the brain images as normal or pathological. Finally, the proposed technique gives a promising result compared to existing methods but failed to classify the large datasets.

In MRI scanning, Zhang, Yudong, et al. (2015) suggested a comprehensive automatic classification technique for separating abnormal from normal brains. First, the stationary wavelet transform (SWT) method was used to extricate the attributes, and then principal component analysis (PCA) was used to reduce the SWT coefficients. Finally, the authors presented the "Generalized Eigenvalue Proximal Support Vector Machine" (GEPSVM) and GEPSVM accompanied by RBL kernel as two classifiers. The proposed methods were tested on three benchmark datasets by running the 10- of K-fold cross-validation. The proposed technique has a classification accuracy of 96.4% which can be used in clinical practice but loss of the tumor details.

To address all the issues in the existing methods in this work, we suggest a flow work for segmentation of brain tumor and classification with high accuracy with minimal loss of tumor information.

3 Methodology

In this paper, the proposed framework is to classify the tumor from T1w MRI images by utilizing the MLT. The fully annotated MRI image database with a size of 256×256 was received from BRATS (Brain Tumor Segmentation), Benchmark 2017 (Masood et al., 2015) and Harvard University dataset for evaluation. This work was run by using MATLAB 2020a with a Core™ i7 (2.5 GHz).

Three modules make up the suggested technique. The system's framework is divided into four primary parts. The manual code for the skull stripping method is used in the first module to remove the undesired parts of the brain tumor images and denoise them utilizing the median filter while keeping the edge information. In the next stage, the denoised pictures were segmented utilizing the C-V active contour technique to obtain the segregated parts in the MRI images. Finally, in the next module, fundamental features were extracted based on GLCM, and essential features were selected using the various statistical parameters.

Algorithms 1 *Algorithm for proposed flow work*

Start	
Begin	
Input	*image I (m, n), where I (m, n) ∈ N*
Output	*Tumorous or Non-tumorous*
1st Step	*For i=1 to Max Count (N (i))*
2nd Step	*Remove skull using BSE (Brain surface extractor)*
3rd Step	*De-noising the image by median filter*
4th Step	*i= i+1*
5th Step	*End for*
6th Step	*Images segmented by using CVS and LSS*
7th Step	*Image features extracted by GLCM*
8th Step	*Images classified by KNN and SVM.*
9th Step	*Output image ⟶ Tumorous or not*
End	

The last module is a classification which is essential to classify the tumor region irrespective of normal brain image by considering the KNN and SVM classifiers. The intended flow diagram for the detection of brain tumor and classification from the selected MRI image is shown in Fig. 1. The proposed work intended for accurate tumor segmentation without loss of tumor details and effectively classifying the tumor whether tumorous or non-tumorous. The proposed system in terms of the algorithm given in stepwise above (Algorithm 1) and key element details are provided briefly in the subsections.

3.1 Tumor preprocessing

Preprocessing is required since it improves some of the image attributes that are necessary for future processing. The skull has no information about a tumor that can be physically removed or removed using various skull stripping procedures (brain extraction tool-BET) to save time in processing the undesirable region. The noise in brain MRI images is then removed using a median filter (Khan et al., 2019). The median filter is a nonlinear filter that reduces noise from level two while keeping tumor edge information. As a result, we recommend the median filter for denoising following skull stripping in our study over others.

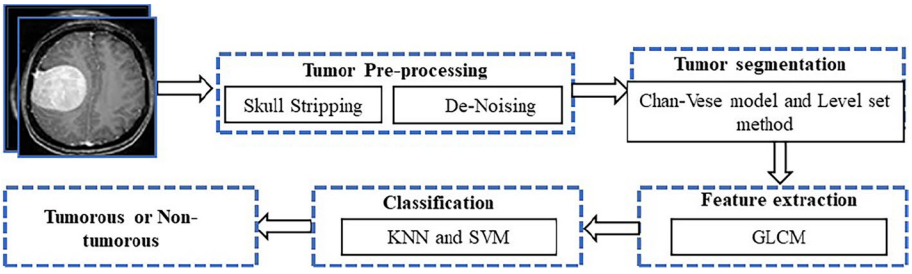

Fig. 1 The proposed flow diagram of brain tumor segmentation and classification

3.2 Tumor segmentation

Image segmentation divides a digital image into several parts in computer vision (pixel sets, also known as image objects). The goal of segmentation is to make an image's representation more meaningful and easier to examine by simplifying and/or changing it. Image segmentation is frequently used to determine objects and boundaries in pictures (lines, curves, etc.). Picture segmentation, in particular, is a way of giving a label to each pixel in an image so that pixels with the same label have comparable features (Manjula et al., 2020).

Chan-Vese segmentation (CVS) model: The C-V model exhibited in complex forms is incredibly efficient in packing a wide range of images, including those challenging to section using current division techniques. Threshold values and gradient-based algorithms are common approaches. The segmentation is used to acquire the information of the tumor from the preprocessed test image. In this work, we use a semiautomated CVS technique to mine the tumor part (Menze, 2017; Nagajaneyulu & Satya Prasad, 2020). The CVS is initiated with a bounding box, and the box can converge in the direction of the tumor area. This convergence will identify all possible similar pixel groups of the tumor segment, and the CVS stops its confluence when the energy function of the CVS model reaches a minimal value.

Level-set segmentation (LSS) method: The method of level set is often used to capture interface generation, mainly when topological changes occur. "Over the previous few decades, the LSS method has been utilized to segment images. Surfaces or contours are a collection of a set of higher-dimensional functions at the zero levels termed a level-set function (Manjula et al., 2020). It can be used to represent surfaces or contours with complicated topologies and inherently change their topology shape." The segmentation problem is solved using partial differential equations and the Hamilton Jacob method.

Image I, which can be modeled as in Eq. (1), is used to deal with the strength of inhomogeneity.

$$I = b_1 J_1 + N_1 \tag{1}$$

When N_I is "AWGN," "J_I" is an input refinement constant, and "b_1" is a bias field approximation constant (Manjula et al., 2020; Nagajaneyulu & Satya Prasad, 2020).

3.3 Feature extraction

When input data is enormous, its information may be redundant, so reduce to required data extracted by converting higher-dimensional data into a feature vector set. This module extracts the critical elements as are necessary for image categorization. The texture characteristics are generated from the segmented picture depicting the image's texture property, a segmented brain MR image. Because GLCM is a robust, high-performance method, it is used to extract these properties.

The extraction method of the GLCM texture function is very competitive because the use of a smaller number of gray levels reduces the size of the GLCM, reducing the algorithm's computational cost and retaining high classification rates at the same time (Yousefi et al., 2014). To differentiate the images of normal and abnormal brains, these GLCM features are used. The texture contains crucial information about the structure of the surface. Textural characteristics based on gray-tone spatial relationships can be used to classify

images in general (Sai Deepthi et al., 2019). Texture features are used in medical imaging to examine lesions or tumors since they are considered a surface attribute of the tumor. Each tumor has its representation in statistical texture. Two methodologies are employed to calculate the texture features: structured and statistical. Second-order statistical features are extracted using the method given. Contrast, correlation, uniformity, and homogeneity are four texture properties that are extracted. One of the main reasons for choosing only four attributes is to choose the most reliable data.

The suggested method extracts geometric properties, also known as shape features, from the entire dataset. The goal of geometric feature extraction in this study is to determine the shape particulars of the tumor region. As a result, nine geometric properties, including area, filled area, circularity, perimeter, orientation, extension, solidity, major axis length, and minor axis length, are retrieved (Sharif et al., 2019). Then, for each image, these parameters are computed one by one from regions of segmented tumor. The primary goal of extracting these features is to gather tumor geometry information, which is then fused into texture features for improved classification accuracy (Manjula et al., 2020; Nagajaneyulu & Satya Prasad, 2020; Yousefi et al., 2014).

Later, a two-tailed *t*-test feature selection technique is employed to select the leading features based on the p-value attained during the statistical test. The feature selection further helps to reduce the complexity during the training and testing of the classifier and helps to achieve better classification accuracy (Sai Deepthi et al., 2019).

3.4 Classification

Various classifiers, like naive Bayes, logistic regression, random forest, decision tree, etc., are considered. The logistic regression works only predicted variable is binary and the naïve Bayes fast but bad estimator (Siva & Bojja, 2019). The decision tree is unstable due to slight variations in the data. The random forest is complex and difficult to implement but reduces the overfitting problem. Based on the literature, the KNN and SVM provide the promising results. So, in proposed flow work, we preferred KNN and SVM for classification purpose. The two or multilevel classifier plays a crucial function in the MLT (Sreelakshmi & Inthiyaz, 2019) and several earlier works confirm the need for the classifiers. The accuracy depends on the feature extracting actions employed to mine the essential features from the MRI and the feature selection procedure adopted to recognize the dominant features.

- To train and classify input features, SVM is employed. There are also other SVM families, including the kernel, box constraint, and auto-scale. Kernel functions were chosen because of their widespread use; they include polynomial, linear, and Gaussian radial basis GRB functions (Sampath Dakshina Murthy et al., 2019). SVM parameters used in the model are RBF kernel, C—regularization parameter, and $C = 10$ in the model. Gamma is a kernel coefficient used in the RBF kernel gamma here taken as 1/n features (Harish et al., 2019; Sampath Dakshina Murthy et al., 2019; Sreelakshmi & Inthiyaz, 2019).
- KNN: "Feature similarity" is used to forecast the values of new data points, suggesting that the new data point will be assigned a value based on how closely it resembles the issues in the training set. Because it stores all of the training data, it is a computationally expensive algorithm. In comparison with other supervised learning methods, this one requires a lot of memory capacity. In the event of an enormous N, prediction is

slow. In addition, it is susceptible to data scale and irrelevant factors (Koteswara et al., 2019; Vamsidhar et al., 2019).

There is no organized technique to locate the best incentive for "K". We need to discover different qualities by experimentation and expecting that preparation information is obscure. Choosing more modest qualities for K can be uproarious and will affect the outcome. More significant estimations of K will have smoother choice limits which mean lower fluctuation, however, expanded predisposition, likewise, computationally costly (Sreedhar & Bojja, 2019).

Another approach to pick K is, however, cross-approval. One approach to choose the cross-approval dataset from the preparation dataset. Take the little part from the preparation dataset and consider it an approval dataset, and afterward utilize the equivalent to assess various potential estimations of K (Bashar, 2019; Malakonda et al., 2019). This way we will foresee the mark for each occurrence in the approval set utilizing with K equivalents to 1, K equivalents to 2, K equivalents to 3, and afterward, we see what estimation of K gives us the best exhibition on the approval set and afterward, we can take that worth and utilize that as the last set of our calculation, so we are limiting the approval mistake. When all is said in done, work on, picking the estimation of k will be $k = \text{sqrt}(N)$, where N denotes the number of tests in your preparation dataset (Vijayakumar et al., 2020). Try and keep the estimation of k odd to stay away from disarray between two classes of information. The parameters used are Minkowski, $K = 7$, Hyperparameter p, if set $p = 1$, leaf size = 5, best neighbors = 7 [32].

4 Results and discussion

In this segment, the results are described in terms of performance measures. We have selected some malignant (cancerous) and benign (non-cancerous) tumors from these datasets for segmentation and classification. The proposed flow work is validated on two datasets, including BRATS 2017 dataset and Harvard medical images. T1-weighted MR brain images in the axial plane with a resolution of 1 mm^3 make up the BRATS 2017 dataset. It has a 1 mm slice thickness, 3% noises (estimated due to the bright tissue), and 20% intensity non-uniformity in its T1 modality (RF). This dataset (dataset-66) has 152 photographs with a size of 256×256 pixels. The sample and preprocessed images of selected datasets are depicted in Fig. 2. The denoised images are portioned into isolated regions by using the global-based segmentation technique that is the CVS model. The outcomes of both the CVS model and LSS method are compared in terms of similarity index measures. In addition, GLCM features are deliberated from an image which is binary segmented. Both KNN and SVM classification methods are used for the framework evaluation. The accomplishment of these methods is assessed by four metrics: accuracy, specificity, sensitivity, and precision.

The evaluations are split into two parts. First, the findings of the segmentation are addressed in terms of the Jaccard similarity index (JSI), dice coefficient (DC), and structural similarity index measure (SSIM). The area and the number of pixels are found in the first phase. The classification results are then generated in the second stage, with SVM serving as the leading classifier, and its performance is compared to that of k nearest neighbors (KNN). The accuracy, specificity, sensitivity, accuracy, false-negative rate (FNR),

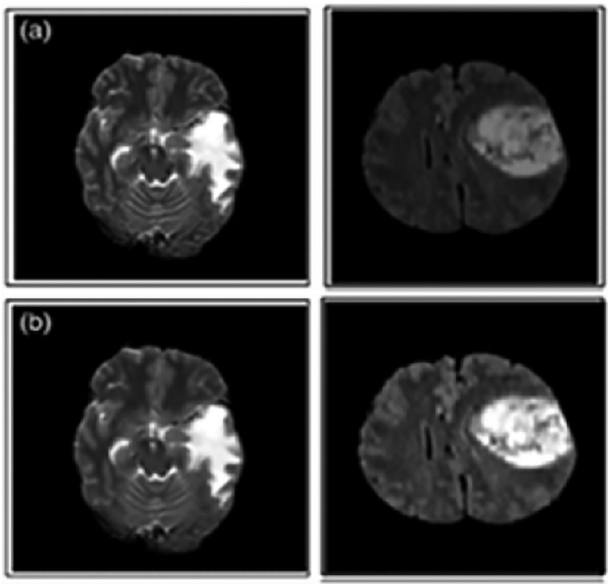

Fig. 2 The sample and preprocessed images (**a**) skull stripped original images and below row (**b**) denoised images

false-positive rate (FPR), negative predictive value (NPV), and positive predict value (PPV) of these classification algorithms are all measured.

4.1 Results of segmentation

This section analyzes the results of segmentation and to check the authenticity of active contour models (ACM), such as the CVS model and the LSS method. Three parameters, including JSI, DC, and SSIM, are calculated to examine the performance. The performance evaluation metrics are briefly explained below:

Dice coefficient: "The dice coefficient is used to find the degree of similarity between the mined tumor and the manually or expert segmented tumor" (Hasane et al., 2019).

$$\text{Dice}(X,\ Y)\ =\ 2 * \frac{|X_1 \wedge Y_1|}{(|X_1| + |Y_1|)} \tag{2}$$

$1 \rightarrow X$ and Y Overlap.

$0 \rightarrow X$ and Y do not overlap.

Structural similarity index measure (SSIM): It indicates the deterioration of image quality due to data compression, and the expression is given in Eq. (3), as shown below

$$\text{SSIM}(x, y) = \frac{(2\mu_x\mu_y + c_1)(2\sigma_{xy} + c_2)}{(\mu_x^2\mu_y^2 + c_1)(\sigma_x^2 + \sigma_y^2 + c_2)} \tag{3}$$

where μ *is* mean, σ is variance and σ is the covariance. The c are constants. A higher SSIM value is needed for good contrast and luminance (Hasane Ahammad & Rajesh, 2018).

Jaccard similarity index: It calculates the degree of similarity between two pieces of data (Si & De, 2018).

$$\text{JSI} = J(X, Y) = \frac{|X \cap Y|}{|X \cup Y|} = \frac{|X \cap Y|}{|A| + |B| - |A \cap B|} \tag{4}$$

where *X and Y* imply the detected region and original region. Higher values indicate better performance (Ahilan & Manogaran, 2019).

In comparison with the LSS method, "the C-V model is based on the Mumford-shah segmentation function and energy minimization, which is used to solve the problem easily. The C-V model is efficient in contour detection. The segmented output images along with selected images from BRATS 2017 as shown in Fig. 3." As per Fig. 3, the CVS method segments the tumor part from preprocessed images exactly with proper information as compared with the LSS method. The LSS method requires human interaction and difficult to initialize the initial position of the tumor. The CVS method globally accepted to semisupervised brain tumor segmentation.

Twenty brain tumor photographs are picked from both datasets segmentation results were obtained. The size or volume of the tumor depends on its benign (< 2 cm) or malignant (> 5 cm), but in this work we are selected abnormal images that sizes do not matter, so proposed flow work can segment any size of tumor from MRI images.

Their ground truth images calculate the selected parameters. An expert doctor designs the ground truth images of the Harvard dataset and the ground truth images of the BRATS 2017 dataset are available with the same downloaded file. The performance of CVS and LSS is assessed with analysis between the segmented tumor and ground truth and the essential values are then computed as presented in Table 1. For this purpose, we are applied on two high-quality images from both datasets and recorded them accordingly (Fig. 4).

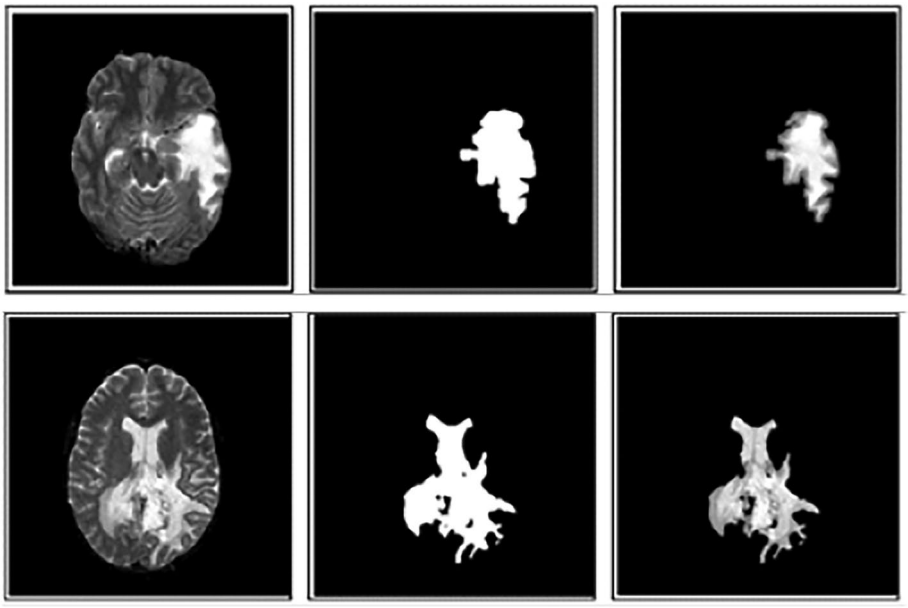

Fig. 3 Results for segmentation (BRATS 2017 dataset) **a** preprocessed, **b** CVS segmented images, and **c** LSS segmented images

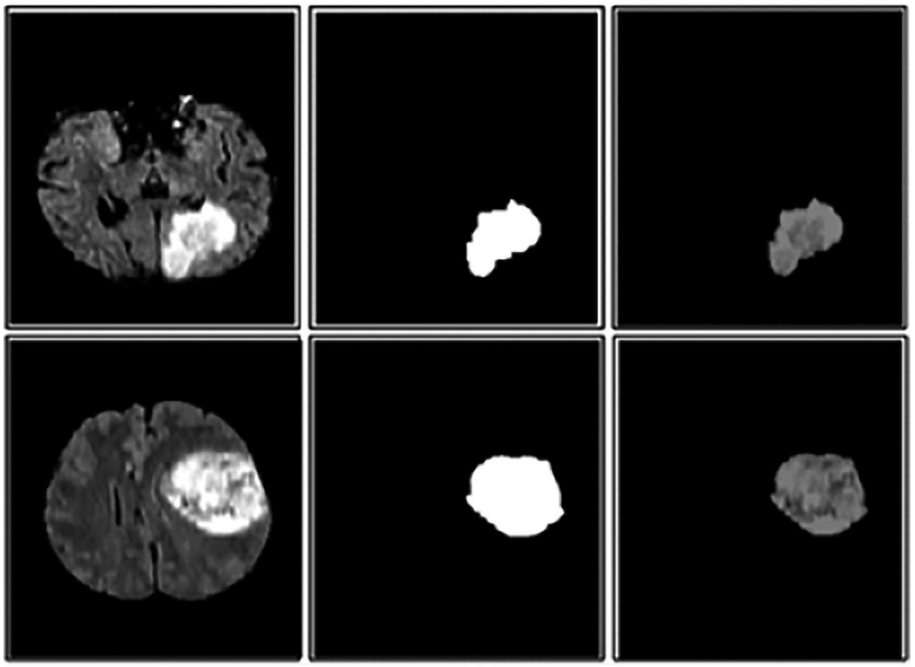

Fig. 4 Results for segmentation (Harvard University dataset **a** preprocessed image, **b** CVS segmented images, and **c** LSS segmented images

Table 1 Image similarity measures attained by ACM models

Dataset	Images	Method	JSI	DC	SSIM
BRATS 2017	01	LSS	0.8991	0.9469	0.9819
		CVS	0.9423	0.9631	0.9966
	02	LSS	0.9145	0.9537	0.9894
		CVS	0.9531	0.9732	0.9987
Harvard	03	LSS	0.8868	0.9412	0.9613
		CVS	0.9213	0.9621	0.9713
	04	LSS	0.8668	0.9381	0.9780
		CVS	0.9197	0.9501	0.9816

Here, the only similarity with the ground truth image is measured rather than other parameters. The JSI, DC, and SSIM values are calculated and recorded in Table 1 for ACM models on both datasets, respectively.

The bar graph is plotted for JSI values obtained by both LSS and ACS on selected datasets, shown in Fig. 5.

The metrics of segmentation results for BRATS 2017 datasets are given in Table 1, having average JSI as 0.9068 to LSS method and 0.9477 to CVS model, respectively. Following that, using ground truth images, the same parameters were estimated for the Harvard

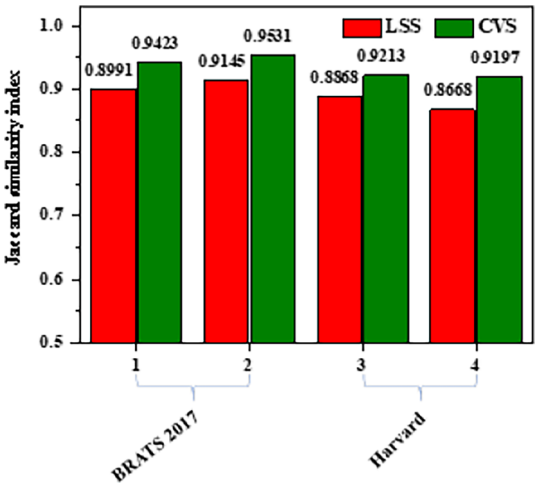

Fig. 5 Comparison of JSI for LSS and CVS model on both datasets

dataset, yielding average JSI values of 0.8768 for the LSS technique and 0.9205 for the CVS model, respectively. Finally, in the same manner, DC and SSIM values are calculated for both datasets.

From all the performance measures, it is observed that the proposed CVS model performed better on BRATS 2017 dataset as compared to the Harvard dataset. Moreover, a comparison was conducted for the BRATS 2017 dataset with existing methods for average JSI values as given in Table 2. The CVS model in the proposed framework gives the on average 94.77% of JSI over the existing methods. The highest JSIs attained by existing techniques 88.90 and 94.00% only.

4.2 Classification results

Next, using the GLCM, the features have been extracted. After extracting the tumor from the 300 MRI slices of T1w images, the texture and the shape features are then extracted using the GLCM method, eight dominant features are chosen with a *t*-test, and the selected features and its statistical values. In this work, we concentrate on the classification of the detected tumor, whether tumorous or non-tumorous. So, the next classifiers are applied based on extracted features of the tumor and non-tumor images.

Data preparation: The performance of the classifier is based on the data considered during the training and testing task. In this work, out of 300 images, 210 images (70%) are used to train, 90 images (30%) for validation are considered to test the classifier. The classification results are validated on BRATS 2017 dataset which consist of both healthy and unhealthy images. All the results calculated using tenfold cross-validation.

Table 2 Comparison of JSI on BRATS 2017 dataset with presently existing techniques

Methods	Technique	JSI Average
Avina-Cervantes et al. (2018)	Multilevel Otsu	0.8890
Benson et al. (2016)	Mathematical morphology	0.9400
Proposed flow work	Chan-vese segmentation model	0.9477

Table 3 Performance evaluation of SVM and KNN classifiers

Classifier	FPR	FNR (%)	Specificity (%) Sensitivity (%)	NPV (%)	PPV (%)	Accuracy (%)
SVM	0.023	1.87	97.09 97.99	98.94	99.97	98.13
KNN	0.057	7.70	93.99 84.69	91.75	93.93	92.30

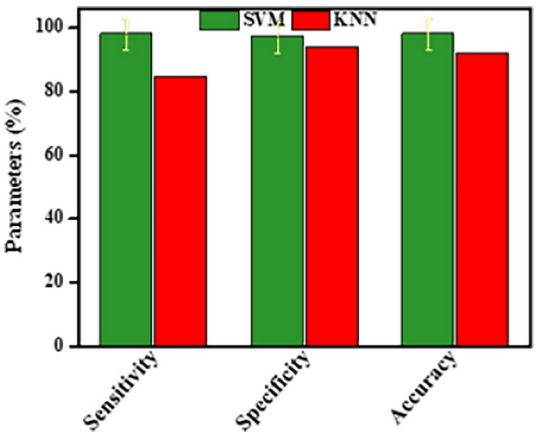

Fig. 6 Comparison of performance measures for SVM and KNN classifier on BRATS 2017 dataset

The performance measures obtained with both SVM and KNN for "$\sigma = 1.4$" are shown in Table 1. When the number of chosen features is 8 and $\sigma = 1.4$, the SVM classifier performance is superior. For lesser and higher values of the chosen features, the accuracy attained is less. So, same number of selected features are given as input, and parameters are calculated.

Hence, in the framework of MLT, the SVM is trained and tested with 8 dominant features along with $\sigma = 1.4$ is considered. The performance of SVM is then compared against KNN. In Table 3 the performance values of the results are listed. As per the table, the sensitivity, specificity, and accuracy values obtained with KNN are 84.69, 93.99, and 92.3%, respectively. The sensitivity, specificity, and accuracy values obtained with SVM are 97.99, 97.09, and 98.13%, respectively. The comparison of performance measures of both SVM and KNN classifier is presented in Fig. 6. As per literature survey, the SVM classifier without active contour segmentation models provides only 96. 48% of classification accuracy for BRATS 2017 dataset. As per comparison of performance metrics such as accuracy, sensitivity, and specificity indicated that the SVM classifier is better to categorize the brain tumor images than the KNN classifier. The SVM technique classifies the tumorous or non-tumorous with an improvement of 5.83% of accuracy as compared with the KNN classifier.

5 Conclusions and future scope

This work aims to present automated brain tumor classification and detection of brain MRI images into cancerous or non-cancerous tumors using the MLT. The introduced flow work has a preprocessing step to remove skull and noise from original images, the

preprocessed images were segmented with C-V model to detect the tumor, GLCM feature extraction for the extraction of important features from segmented, feature selection with two-tailed t-test, training and finally classify the images based on extracted feature selection by employing the SVM and KNN. The C-V model detects the tumor accurately and texture and shape features were extracted by GLCM. Finally based on the attained p-value, an SVM and KNN classifiers were applied to classify the given images whether timorous or non- timorous. The performance of both classifiers measured in terms of accuracy, sensitivity, specificity, and precision. As per outcomes, the SVM outer performs with above 98% of accuracy than the KNN classifier. Finally, the proposed MLT gives better results in the detection and classification of brain tumors and performs better than existing methods. The main limitation in the work is that the SVM cannot handle a larger dataset; hence, when the dataset increases then there is a need for a better classification model. There is also a need for better tuning parameters to be implemented while training the SVM so that we can reduce the computational time.

In the future, this work may be extended toward detecting and classifying the brain tumor more accurately using deep learning techniques on large datasets. This work may implement toward optimization-based segmentation techniques to reduce the time complexity.

References

Ahilan, A., Manogaran, G, (2019). Segmentation by Fractional Order Darwinian Particle Swarm Optimization Based Multilevel Thresholding and Improved Lossless Prediction Based Compression Algorithm for Medical Images, IEEE ACCESS.

Avina-Cervantes, J. G., Cruz-Duarte, J. M., Rosales-Garcia, J., Correa-Cely, C. R., & Garcia-Perez, A. (2018). A closed form expression for the Gaussian–based Caputo–Fabrizio fractional derivative for signal processing applications. *Communications in Nonlinear Science and Numerical Simulation, 61*, 138–148.

Bashar, A. (2019). Survey on evolving deep learning neural network architectures. *Journal of Artificial Intelligence, 1*(02), 73–82.

Benson, C. C., Lajish, V. L., & Rajamani, K. (2016). A novel skull stripping and enhancement algorithm for the improved brain tumor segmentation using mathematical morphology. *International Journal of Image, Graphics and Signal Processing, 8*(7), 59.

Bresson, X., Esedoglu, S., Vandergheynst, P., Thiran, J., & Osher, S. (2007). Fast global minimization of the active contour/snake model. *Journal of Mathematics Imaging Vision, 28*(2), 151–167.

Chakraborty, K., Si, T., De, A., & Sharma, S. K. (2018). Clustering techniques for segmentation of soft tissue sarcoma in MR images. *Journal of Advanced Research in Dynamical and Control Systems, 10*(11), 288–294.

Chan, T. F., Esedoglu, S., & Nikolova, M. (2006). Algorithms for finding global minimizers of image segmentation and denoising models. *SIAM Journal of Applied Mathematics, 66*(5), 1632–1648.

Ersoz, I., et al. (2017). PCA Based clustering for Brain tumor segmentation of T1w MRI images. *Computer Methods and Programs in Biomedicine, 140*, 19–28.

Harish Babu G., Venkatram N., & Kavya M. (2019). Dark channel prior based image dehazing using different transmission map refinement methods. *International Journal of Innovative Technology and Exploring Engineering, 8* 8(12), 3015–3020.

Hasane Ahammad, S. K., & Rajesh, V. (2018). Image processing-based segmentation techniques for the spinal cord in MRI. *Indian Journal of Public Health Research and Development, 9*(6), 317–323.

Hasane Ahammad S., Rajesh V., Hanumatsai N., Venumadhav A., Sasank N.S.S., Bhargav Gupta K.K., & Inithiyaz S. (2019) MRI image training and finding acute spine injury with the help of hemorrhagic and non-hemorrhagic rope wounds method. *Indian Journal of Public Health Research and Development, 10*(7), 404–408

Luxit Kapoor & Sanjeev Thakur. (2017). A Survey on Brain Tumor Detection Using Image Processing Techniques. *Proceedings of 7th international conference on Cloud Computing, Data Science & Engineering – Confluence*, Jan 12–13; Noida, India, pp 582–585.

Muhammad A. Khan, Ikram U. Lali, & Amjad Rehman et al. (2019). Brain tumor detection and classification: A frame-work of marker-based watershed algorithm and multilevel priority features selection. *Microscopy Research and Technique*, pp 1–14, https://doi.org/10.1002/jemt.23238.

Koteswara Rao L., Rohni P., & Narayana M. (2019). Lemp: A robust image feature descriptor for retrieval applications. *International Journal of Engineering and Advanced Technology, 9*(1), 4565–4569.

Lankton S., A., & Tannenbaum (2008). Localizing region-based active contours. *IEEE Transaction Image Processing, 17* (11), 2029–2039.

Li, C., Huang, R., Ding, Z., Gatenby, J. C., Metaxas, D. N., & Gore, J. C. (2011). A level set method for image segmentation in the presence of intensity inhomogeneities with application to MRI. *IEEE Transactions on Image Processing, 20*(7), 2007–2016.

Liu, J., Li, M., Wang, J., Wu, F., Liu, T., & Pan, Y. (2014). A survey of MRI-based brain tumor segmentation methods. *Tsinghua Science & Technology., 19*(6), 578–595.

Malakonda Reddy B., & Zia Ur Rahman M. (2019). Analysis of SAR images using new image classification methods. *International Journal of Innovative Technology and Exploring Engineering, 8* (8), 760–764.

Manjula, K. T., et al. (2020). Brain tumor segmentation by level-set and Chan-Vese methods using different fusion approaches. *International Journal of Emerging Trends in Engineering Research (IJETER), 8*(3), 769–775.

Masood, S., et al. (2015). A Survey on Medical Image Segmentation. *Current Medical Imaging Reviews, 11*(1), 3–14.

Menze et al., (2017). The Multimodal Brain Tumor Image Segmentation Benchmark (BRATS). *IEEE Transactions on Medical Imaging*.

Nagajaneyulu, P. V., & Satya Prasad, K. (2020). Performance analysis of CNN fusion-based brain tumor detection using Chan-Vese and level set segmentation algorithms. *International Journal of Signal and Imaging Systems Engineering , 12* (1–2), 62–70.

Nagajaneyulu, P. V., & Satya Prasad, K. (2020). Brain tumor segmentation of T1w MRI images based on clustering using dimensionality reduction random projection technique. *Current Medical Imaging, 17* (3), 331–341. https://doi.org/10.2174/1573405616666200712180521.

Rohini1ana, P. V., & Pushpa ani, M. (2015). Analysis and Detection of Brain Tumor Using Image. *Processing Technique. International Journal of Advanced Technology in Engineering and Science, 3* (1), 393–399.

Raju K., Pilli S.K., Kumar G.S.S., Saikumar K., & Jagan B.O.L. (2019). Implementation of natural random forest machine learning methods on multispectral image compression. *Journal of Critical Reviews, 6* (5), 265–273.

Remya Ajai A.S., & Gopalan S. (2020). Analysis of Active Contours Without Edge-Based Segmentation Technique for Brain Tumor Classification Using SVM and KNN Classifiers. In: Jayakumari J., Karagiannidis G., Ma M., Hossain S. (eds) Advances in Communication Systems and Networks. Lecture Notes in Electrical Engineering, vol 656. Springer, Singapore. https://doi.org/10.1007/978-981-15-3992-3_1

Sai Deepthi, U., Sudha Madhuri, A., Sai Prasad, P. (2019). Comparative analysis of brain tumor detection using deep learning methods. *International Journal of Scientific & Technology Research, 18* (12), 250–254, ISSN:2277–8616

Sampath Dakshina Murthy A., Satyanarayana Murthy P., Rajesh V., Hasane Ahammad S., & Omkar Lakshmi Jagan B. (2019). Execution of natural random forest machine learning techniques on multispectral image compression. I*nternational Journal of Pharmaceutical Research, 11* (4), 1241–1255.

Sharif, M. I., et al. (2019). Active deep neural network features selection for segmentation and recognition of brain tumors using MRI images. *Pattern Recognition Letters, 129*, 181–189.

Si, T., De, A., Bhattacharjee, A. K. (2018). Segmentation of Brain MRI Using Wavelet Transform and Grammatical Bee Colony. *Journal of Circuits, Systems and Computers*.

Siva D., & Bojja P. (2019). MLC based classification of satellite images for damage assessment index in disaster management. *International Journal of Advanced Trends in Computer Science and Engineering, 8* (6), 2825–2830.

Sreedhar Babu S., & Bojja P. (2019). Machine learning algorithms for MR brain image classification. *International Journal of Recent Technology and Engineering, 8*(3), 6744–6747.

Sreelakshmi D.,& Inthiyaz S. (2019). 'A review on medical image denoising techniques. *International Journal of Scientific and Technology Research, 8*(11), 1883–1887.

Vamsidhar, E., Jhansi Rani, P., & Rajesh Babu, K. (2019). Plant disease identification and classification using image processing. *The International Journal of Engineering and Advanced Technology, 8* (3), 442–446.

Vijayakumar, T.,& Vinothkanna, R. (2020). Mellowness detection of Dragon fruit using deep learning strategy. *Journal of Innovative Image Processing (JIIP) 2* (01), 35–43.

Viji, KS Angel, & Hevin Rajesh, D. (2020). An efficient technique to segment the tumor and abnormality detection in the brain MRI images using KNN classifier. *Materials Today: Proceedings, 24* 1944–1954.

Siamak Yousefi, Michael H. Goldbaum, Linda M. Zangwill, Felipe A. Medeiros, & Christopher Bowd (2014). Recognizing Patterns of Visual Field Loss Using Unsupervised Machine Learning; Proceedings of SPIE 2014; March 21; 90342M. https://doi.org/10.1117/12.2043145.

Zhang, Yudong, et al. (2015). Magnetic resonance brain image classification via stationary wavelet transform and generalized eigenvalue proximal support vector machine. *Journal of Medical Imaging and Health Informatics, 5* (7), 1395–1403.